F2,6BP restores mitochondrial genome integrity in Huntington's Disease

Anirban Chakraborty[a], Santi M. Mandal[b], Mikita Mankevich[b], Sravan Gopalkrishnashetty Sreenivasmurthy[c], Muralidhar L. Hegde[d], Balaji Krishnan[c], Gourisankar Ghosh[b*], Tapas Hazra[a*]

[a]Department of Internal Medicine, University of Texas Medical Branch, Galveston, TX, 77555, USA
[b]Department of Chemistry and Biochemistry, University of California San Diego, LA Jolla, California 92093, USA
[c]Department of Neurology, University of Texas Medical Branch, Galveston, TX, 77555, USA
[d]Department of Neurosurgery, Center for Neuroregeneration, The Houston Methodist Research Institute, Houston, Texas 77030, USA

*Address correspondence to:

Tapas Hazra
Department of Internal Medicine-Pulmonary, Critical Care & Sleep Medicine
University of Texas Medical Branch, Galveston, TX 77555, USA
Tel: (409) 772-6308
Fax: (409) 747-8608
E-mail: tkhazra@utmb.edu

Gourisankar Ghosh
Department of Chemistry and Biochemistry,
University of California San Diego, LA Jolla, California 92093, USA
Tel: (858) 822-0469
E-mail: gghosh@ucsd.edu

Keywords: DNA strand break repair, mitochondria, PNKP, Huntington's disease, Fructose-2,6-bisphosphate

Abstract

Several reports have indicated that impaired mitochondrial function contributes to the development and progression of Huntington's disease (HD). Mitochondrial genome damage, particularly DNA strand breaks (SBs), is a potential cause for its compromised functionality. We have recently demonstrated that the activity of polynucleotide kinase 3'-phosphatase (PNKP), a critical DNA end-processing enzyme, is significantly reduced in the nuclear extract of HD patients due to lower level of a metabolite fructose-2,6 bisphosphate (F2,6BP), a biosynthetic product of 6-phosphofructo-2-kinase fructose-2,6-bisphosphatase 3 (PFKFB3), leading to persistent DNA SBs with 3'-phosphate termini, refractory to subsequent steps for repair completion. PNKP also plays a pivotal role in maintaining mitochondrial genome integrity. In this report, we provide evidence that both PFKFB3 and F2,6BP, an allosteric modulator of glycolysis, are also present in the mitochondria. Notably, the level of F2,6BP, a cofactor of PNKP, is significantly decreased due to the degradation of PFKFB3 in the mitochondrial extract of HD patients' brain. PNKP activity is thus severely decreased in the mitochondrial extract; however, addition of F2,6BP restored PNKP activity. Moreover, supplementation of F2,6BP in HD mouse striatal neuronal cells restored mitochondrial genome integrity and partially restored mitochondrial membrane potential and prevented pathogenic aggregate formation. We observed similar restoration of mitochondrial genome integrity in HD drosophila supplemented with F2,6BP. Our findings, therefore, suggest that F2,6BP or its structural analog hold promise as a therapeutic for restoring both nuclear and mitochondrial genome integrity and thereby of organismal health.

Introduction

Huntington's disease (HD), a devastating hereditary neurological disorder, is caused by toxic expansion of the polyglutamine (polyQ) stretch in the N-terminus of huntingtin protein (HTT)[1]. HD is inherited, and is considered as monogenic disease; however, pathogenesis is highly complex. Genome-wide association studies showed a strong correlation between DNA repair deficiency and the age-dependent onset of HD[2,3]. In addition to nuclear genome damage, recent advances in mitochondrial research implicated previously unanticipated roles for mitochondria in human diseases, particularly aging and neurological disorders, including HD[4-7]. Mitochondrial DNA (mtDNA) damage is a potential cause of mitochondrial dysfunction in HD. The mitochondrial genome is subjected to continuous insult by endogenous reactive oxygen species (ROS) because of its proximity to the site of ROS generation via mitochondrial electron transport system complexes. Furthermore, mtDNA lacks protective histones, unlike nuclear DNA (nDNA), and so it is more susceptible to oxidative damage[8]. Mitochondria have a high rate of transcription and importantly, most of the mitochondrial genome is transcribed. Thus, compromised mitochondrial DNA repair capacity could contribute to the onset of various neurodegenerative diseases and/or pathologies, including HD[9-11].

To protect mtDNA from ROS induced oxidative damage, a range of DNA repair mechanisms have evolved including base excision repair (BER) and single strand break repair (SSBR)[12]. Polynucleotide kinase 3'-phosphatese (PNKP) is a major enzyme for processing both "non-ligatable" 3'-phosphate (3'-P) and 5'-OH termini at strand breaks in mammalian genomes[13-14]. Several recent reports, including ours, have documented an association of PNKP deficiency with neurological/developmental disorders[15-18]. However, the underlying

biochemical bases of such phenotypes, which are exclusive to the nervous system, are not well understood. We have recently showed that wild-type HTT plays an important role in DNA repair by most likely providing a platform for the assembly of a novel transcription-coupled DNA repair (TCR) complex in nuclei that includes, RNA polymerase II (RNAPII), PNKP and other DNA repair proteins[19-20]. This specialized DNA repair complex repairs DNA lesions during transcription to maintain genome integrity of the neurons, preserving their function and by doing so, extend their survival. We have further demonstrated cell death due to the loss of DNA repair (3'-phosphatase) activity of PNKP, but not its protein level, in HD brain extracts, leading to accumulation of DNA SBs, including double strand breaks[20]. Most importantly, we have observed that PNKP interacts with the nuclear isoform of a glycolytic enzyme, 6-phosphofructo-2-kinase fructose-2,6-bisphosphatase 3 (PFKFB3). Depletion of PFKFB3 markedly reduced PNKP activity without changing its protein level. Notably, the levels of both PFKFB3 and its product fructose-2,6 bisphosphate (F2,6BP), an allosteric modulator of glycolysis, are significantly lower in the nuclear extracts of post-mortem HD patients' brain. Supplementation of F2,6BP in HD mouse striatal neuronal cells and in HD flies fully restored nuclear genome integrity and functionality[20], suggesting F2,6BP to be a positive regulator of PNKP activity *in vivo*.

The repair of ROS-induced DNA SBs in the mitochondrial genome is well characterized. We and others have shown the presence of DNA glycosylases, NEIL1/NEIL2 and PNKP in the mitochondria[21-23]. NEIL1 and NEIL2 initiate BER process by their combined DNA glycosylase and AP lyase activities and creates SBs with 3'-P termini, a substrate for PNKP. Additionally, endogenous DNA strand breaks rarely harbor the canonical 3'-OH and 5'-P and such DNA termini require further processing. One of the major blocked DNA termini in mammalian cells is the 3'-P and such DNA ends, in addition to impeding DNA repair, can stall elongating RNA polymerases, leading to DNA damage response via p53 activation. Thus, processing of such "non-ligatable" 3'-P-containing DNA termini is essential for repair progression and efficient transcription even within mitochondria. Since PNKP, a major 3'-phosphatase in mammalian cells[24], is also present in mitochondria, we, therefore, asked whether activity of PNKP is compromised in mitochondria of HD patients and whether PFKFB3 or F2,6BP has any role in mtDNA repair as we observed earlier for nuclear DNA repair[20]. Surprisingly, we observed that both PFKFB3 and F2,6BP localize to mitochondria and their levels are significantly low in HD patients' mitochondrial extract, leading to abrogated mtPNKP activity. Supplementing F2,6BP in HD-mouse striatal neuronal cells and a Drosophila HD model system[25] restored mitochondrial genome integrity. Overall, our data indicate possibility of exploring the therapeutic potential of the metabolite or its analog in HD or related pathology.

Results and discussion

Mitochondrial PNKP activity is reduced in HD

Our previous studies demonstrated that nuclear PNKP activity is diminished in HD mouse models[19] and post-mortem brain tissues from HD patients[20]. Given that PNKP is known to translocate to mitochondria[22], we investigated whether its activity is also compromised in mitochondria by assessing the PNKP activity in the mitochondrial extracts from the frontal cortex of post-mortem HD brains as compared to age- and gender-

matched healthy controls. Indeed, we observed a marked abrogation of 3'-phosphatase activity of PNKP in HD samples **(Fig. 1A, lanes 6-9 vs lanes 2-5)**.

Since PNKP is an essential DNA end-processing enzyme, we next examined accumulation of DNA SBs in the mitochondrial genome by a long amplicon (LA)-qPCR-based assay using mitochondrial genome specific primers. In this assay, a relative decrease in the PCR product of the long amplicon (~8-10 kb) vs the short amplicon (~250 bp) suggests increased DNA damage, as higher number of lesions in longer templates impedes PCR amplification with greater efficiency. Consistent with the compromised mtPNKP activity, we detected significant accumulation of DNA SBs in the mitochondrial genome of HD brains **(Fig. 1B, lanes 4-6 vs lanes 1-3)**. In summary, our results indicate that similar to nuclear DNA damage in transcribed genes resulting from reduced nPNKP activity, mtDNA also accumulates damage due to a significant reduction in mtPNKP activity in HD pathology.

Diminished PFKFB3 and F2,6BP levels in HD patients disrupt mitochondrial activity

Given that PNKP levels are similar between HD patients and healthy control samples, and that F2,6BP acts as a cofactor of PNKP to maintain its activity in the nucleus, we postulated that a similar regulatory mechanism might be present in mitochondria. To assess the role of PFKFB3 and its product F2,6BP in mitochondrial DNA repair, we first tested whether PFKFB3 is localized in mitochondria in HEK293 cell line. Indeed, we detected significant amounts of PFKFB3 in the pure mitochondrial extract of HEK293 cells **(Fig. 2A)**. We further confirmed the presence PFKFB3 in the mitochondrial extract from WT mouse striatal neuronal (Q-7) cells and post-mortem frontal cortex from healthy controls **(Fig. 2B, lane 1; Fig. 2C, lanes 1-4)**. To validate these findings, we performed the indirect immunofluorescence and co-staining of mitochondria and nucleus (by Mito tracker green and DAPI, respectively) which confirmed PFKFB3 localization in both the nucleus and mitochondria of Q-7 cells **(Fig. 2D)**. We further observed that mitochondrial integrity was severely compromised in striatal neuronal cells from HD mouse with expanded polyQ repeats (Q-111), with a significant reduction in PFKFB3 levels **(Fig. 2E)**. Western blot analyses also revealed significant decrease in the PFKFB3 levels in the mitochondrial extracts of Q-111 cells **(Fig. 2B, lane 2 vs lane 1)** and HD post-mortem patients' brain **(Fig. 2C, lanes 5-8 vs lanes 1-4)**. The immunostaining revealed a decreased level of nuclear PFKFB3 as well in Q-111 cells, consistent with our previous findings[20]. These observations suggest that the DNA strand break repair components are active in mitochondria of healthy subjects but are compromised under pathogenic conditions. The presence of PFKFB3 in the nucleus and mitochondria further emphasizes its additional function in the DNA repair pathway apart from their function in glycolysis.

We next examined if F2,6BP is present in the mitochondria of healthy individuals and if its level is reduced in the post-mortem HD patients in line with low PFKFB3 levels and PNKP activity. Not only we detected F2,6BP in the mitochondrial extract of healthy subjects, we also found that the level of F2,6BP was nearly 2.5-fold reduced in the mitochondrial extracts of patient samples **(Fig. 2G)**. The level of mtPNKP protein remained comparable in HD patients and their age-matched controls **(Fig. 2C)**. Consistent with our previous observations

in nucleus, the reduction in mtPNKP activity is therefore due to lower levels of F2,6BP and not due to decrease in the level of PNKP[20].

Dysregulated mitochondria in HD

To gain further insight into mitochondrial health and functionality, we measured the mitochondrial membrane potential, a key indicator of mitochondrial health. For this purpose, we utilized tetramethyl rhodamine methyl ester (TMRM) that is readily sequestered in healthy cells with active mitochondria, emitting a red-orange fluorescent signal. Flow cytometry (FACS) analysis revealed a significant decrease in membrane potential in the Q-111 cells relative to Q-7 cells **(Fig. 3A-C)**.

Additionally, we used MitoView™650, a mitochondria specific dye which enables real-time visualization of mitochondrial morphology, distribution, and dynamics in live cells without relying on membrane potential. This dye has an excitation/emission spectrum of 644/670 nm, compatible with the Cy®5 channel. Pure mitochondria were isolated from post-mortem HD brain frontal cortex vs healthy controls, stained with MitoView™650, and analyzed using the 670 nm channel. A single uniform population of mitochondria was found in healthy controls; however, multiple distinct mitochondrial populations were observed in HD samples, which may be attributed to irregular mitochondrial fission or delayed division **(Fig. 3E-G)**. These functional assays underscore that decreased levels of mitochondrial PFKFB3 in HD are associated with compromised mitochondrial health and function.

Exogenous F2,6BP restores PNKP activity and cellular integrity

We investigated the effect of F2,6BP in restoring mtPNKP activity in the mitochondrial extracts based on our previous findings showing that F2,6BP complemented compromised nPNKP activity. F2,6BP was prepared biochemically as described earlier[20] and its effect on the 3'-phosphatase activity of mtPNKP was assessed in mitochondrial extracts. As expected, exogenous F2,6BP restored the 3'-phosphatase activity of PNKP in a dose-dependent manner within mitochondrial extracts from representative post-mortem HD brains (frontal cortex) across different age and gender groups **(Fig. 4A, lanes 5-6 vs lane 4)**. In contrast, related natural metabolites, fructose-6-phosphate (F6P) and fructose 1,6-bisphosphate (F1,6BP) did not restore PNKP activity **(Fig. 4A, lanes 7 and 8)**, highlighting the specificity of F2,6BP in reactivating PNKP. In our previous study, we found compromised PNKP activity in the nuclear extract of Q-111 cells compared to WT cells (Q-7)[20]. Therefore, we assessed PNKP activity in the mitochondrial extracts of Q-7 vs Q-111 cells and observed a reduction in 3'-phosphatase activity in Q-111 cells **(Fig. 4B, lane 3 vs lane 2; lane 7 vs lane 6)**. A similar restoration was observed in mitochondrial extracts from Q-111 cells **(Fig. 4B, lanes 4-5 vs lane 3; lanes 8-9 vs lane 7)**, underscoring F2,6BP's essential role as a co-factor, in enhancing PNKP-mediated DNA repair in mitochondria.

To further evaluate the potential of exogenous F2,6BP in restoring DNA repair deficiency in cellular level, we assessed *in-cell* rescue of genome integrity and functionality in Q-111 cells compared to WT Q-7 cells[26]. F2,6BP was delivered using a non-covalent carrier peptide following an optimized protocol[20] and allowed 72 or 96 hours to alleviate mtDNA damage-induced cellular toxicity. As control, we transfected Q-111 cells with the carrier

peptide alone or with F1,6BP. Importantly, transfection of the peptide alone had no significant toxic effect on mtPNKP activity in either Q-7 or Q-111 cells **(Fig. 5A, lane 3 vs lane 2; lane 5 vs lane 4)**. The restoration of 3'-phosphatase activity of PNKP was observed in a time-dependent manner exclusively in the mitochondrial extracts of F2,6BP-transfected cells **(Fig. 5A, lanes 6-7 vs lane 4)**, but not in cells transfected with either F1,6BP or the carrier peptide **(Fig. 5A, lanes 8-9 or lane 5)**. We also observed significant restoration of mtDNA damage following treatment with F2,6BP, concurrent with rescue of mtPNKP activity **(Fig 5B, lanes 5-6 vs lane 3)**. In our earlier study, we observed a significant increase in the Q-111 cell count following F2,6BP treatment, comparable to control Q-7 cells, contrary to the decreased count under mock treatment (carrier peptide alone) condition[20]. Therefore, our study further indicates that apart from nuclear DNA repair, repair of mtDNA substantially contributes to the rescue of the diseased cells from neurotoxicity and apoptosis.

Exogeneous F2,6BP suppresses HD aggregate formation

Live cell imaging further demonstrated that the treatment with F2,6BP could partially restore the mitochondrial integrity and PFKFB3 level in Q-111 cells consistent with its effect on restoration of PNKP activity and repair of mtDNA damage **(Fig. 2F)**. This restoration was accompanied by a significant increase of mitochondrial membrane potential in Q-111 cells **(Fig. 3D)**.

The polyQ expanded HTT proteins are known to be cleaved at the N-terminus, forming pathogenic aggregates, a hallmark of HD pathology[27,28]. To assess these aggregates, we used Thioflavin-T (ThT), a benzothiazole dye considered a 'gold standard' for detecting neurodegenerative aggregates due to its affinity for β-sheet structures common in pathogenic aggregates. Microscopic analyses following co-staining with ThT and NucRed (a nuclear specific dye) showed significant increase in the aggregation formation in Q-111 cells compared to Q-7 cells **(Fig. 5C, third panel from top)**. Remarkably, F2,6BP treatment substantially reduced aggregate formation in Q-111 cells **(Fig. 5C, third panel from top)**. Similar results were observed when Q-111 cells were stained with a monoclonal antibody that specifically bind to HTT aggregates **(Fig. 5C, top panel)**. Taken together these results indicate a correlation between HTT aggregates, PFKFB3 degradation and impairment of PNKP-mediated DNA strand break repair pathway.

F2,6BP supplementation reverses impaired motor phenotype and mitochondrial DNA damage in Drosophila HD models

In our previous study, we demonstrated that pan-neuronal expression of *Htt*128Q (BDSC# 33808 x 458) resulted in significant impairment of motor neuron function compared to the control used to generate the strains (w^{1118}). When flies were supplemented with F2,6BP for 21 days, vs mock buffer control, motor function was restored, as shown by the climbing assay results[20]. To further investigate whether F2,6BP supplementation would alleviate mitochondrial repair deficiencies, we examined the DNA strand break accumulation in Drosophila mitochondrial genome by LA-qPCR. Flies expressing *Htt*128Q and treated with mock buffer showed elevated level of mtDNA damage **(Fig. 6, lane 2 and 4 vs lane 1),** indicating that the mock buffer could not restore mitochondrial genome integrity. However, significant repair was observed following F2,6BP supplementation and the genome integrity was comparable to the W^{1118} flies **(Fig. 6, lane 3 and 5 vs lane 1)**. These findings confirm the ability of F2,6BP

to specifically reverse the HD neurodegenerative phenotype *in vivo* in neuronal cells by restoring nuclear and mitochondrial DNA repair.

Our previous study demonstrated that PFKFB3, an enzyme traditionally known for its glycolytic function, translocates to the nucleus and participate in nuclear DNA repair via transcription-coupled non-homologous end-joining (TC-NHEJ) pathways[20]. We hypothesized that locally produced F2,6BP is transferred directly to PNKP within the TC-NHEJ complex to potentiate 3'-phosphatase activity of PNKP. This process is severely impaired under HD pathogenic conditions. Our present study provides compelling evidence that PFKFB3 and its product F2,6BP are essential for maintaining mitochondrial PNKP activity, thereby supporting efficient mitochondrial genome repair. Our findings suggest that this repair function of PFKFB3 and F2,6BP is crucial for mitochondrial health and function. Notably, we observed that F2,6BP treatment in cells partially restores mitochondrial integrity, membrane potential and reduces the pathogenic aggregates in neuronal cells expressing polyQ-expanded HTT. It has now been established that PFKFB3 is stabilized during brain excitation[29]. Our results are consistent with this report as it shows that PFKFB3's level is low both in the nucleus and in mitochondria only under pathogenic condition but not in post-mitotic healthy neurons. The mechanistic basis of significantly reduced PFKFB3 protein level in mitochondrial extract from HD patients requires further investigation.

Mitochondria are the sites of cellular energy production. However, recent studies provide evidence of a far wider range of mitochondrial functions. Among these, role of mitochondria in intracellular signaling and in communication with other cellular organelles have been elucidated in various organisms[30]. In particular, stressed mitochondria appear to induce beneficial response through effective mitochondrial-nuclear communication. Our results suggest that a small molecule metabolite, F2,6BP can coordinate such communication by potentiating DNA repair in both these organelles. Currently, no curative therapy is available to halt or reverse HD pathology. Previously, a synthetic small molecule, XJB-5-131 (developed by McMurray's group), a radical scavenger and uncoupler of oxidative phosphorylation, showed promise as a therapeutic compound by suppressing disease phenotypes in HD mouse models[31-32]. Therefore, rescuing diseased cells from oxidative DNA damage could provide a therapeutic approach. Our results in Q-111 cells and in Drosophila provide an avenue of rescue of oxidative stress-induced nuclear and mitochondrial DNA damage through F2,6BP supplementation, concurrent with improved mitochondrial functionality. Thus, our results lay the groundwork for exploring a promising therapeNautic approach through F2,6BP supplementation or its non-toxic analog to prevent key aspects of HD progression by maintaining genomic integrity.

Methods

Cell culture

Human Embryonic Kidney 293 (HEK293; ATCC CRL-1573) cells were grown at 37°C and 5% CO_2 in DMEM: F-12 (1:1, Cellgro) medium containing 10% fetal bovine serum (Sigma), 100 units/ml penicillin, and 100 units/ml streptomycin (Cellgro). Mouse striatum derived cell line from a knock in transgenic mouse containing homozygous Huntingtin (HTT) loci with a humanized Exon 1 containing 7 or 111 polyglutamine repeats (Q-7 and Q-111; Corriell Institute; Cat# CH00097 and CH00095, respectively) were cultured and maintained in Dulbecco

Modified Eagles Medium (high glucose) with 2 mM L-glutamine containing 10% fetal bovine serum, 100 units/ml penicillin and streptomycin, and 0.4 mg/ml G418. Q-111 cells lose the ability to proliferate and survive. Therefore, high-passage numbers were avoided. We routinely tested for mycoplasma contamination in cultured cells using the Mycoalert Mycoplasma Detection Kit (Lonza) according to the manufacturer's protocol, and the cells were found to be free from mycoplasma contamination.

Isolation of mitochondria and mitochondrial extracts from cultured cells and post-mortem human tissues

Mitochondria was extracted from cultured cells and post-mortem tissues using mitochondria isolation kits from Thermo Fischer (Cat# 89874 and 89801). Isolated mitochondria were washed with PBS, treated with trypsin (1 mg/ml in PBS) for 15 min at room temperature to remove contaminating proteins adhered to the outer surface of mitochondria, and then extensively washed with PBS. The washed mitochondria were lysed in 50 mm Tris, pH 7.5, 150 mm NaCl, 1 mm EDTA, 1 mm DTT, and 1% Triton X-100 to prepare purified mitochondrial extract.

Immunoblotting

The proteins in the mitochondrial extracts were separated onto a Bio-Rad 4-20% gradient Bis-Tris Gel, then electro-transferred on a nitrocellulose (0.45 µm pore size; GE Healthcare) membrane using 1X Bio-Rad transfer buffer. The membranes were blocked with 5% w/v skimmed milk in TBST buffer (1X Tris-Buffered Saline, 0.1% Tween 20), then immunoblotted with appropriate antibodies [PNKP (BB-AB0105, BioBharati Life Science), PFKFB3 (GTX108335, GeneTex), COX4 (GTX114330, GeneTex)]. The membranes were extensively washed with 1% TBST followed by incubation with anti-isotype secondary antibody (GE Healthcare) conjugated with horseradish peroxidase in 5% skimmed milk at room temperature. Subsequently, the membranes were further washed three times (10 min each) in 1% TBST, developed using ECL™ Western Blotting Detection Reagents (RPN2209, GE Healthcare) and imaged using Kwikquant image analyzer and image analysis software (ver 5.2) (Kindle Biosciences). Cytosolic and nuclear extracts were prepared as described earlier[20] and their purity were checked by immunoblotting with GAPDH (BB-AB0060 BioBharati Life Science) and HDAC2 (GTX109642, GeneTex) antibodies, respectively.

Human tissue samples

Deidentified human post-mortem frontal cortex tissue of HD patients (PMID: 39298485) and age-matched controls (IRB exempt) were obtained from the biorepository of the Michigan Brain Bank, USA through Materials Transfer Agreement (UTMB 22-UFA00474).

Assay of 3'-phosphatase of mtPNKP

The 3'-phosphatase activity of PNKP in the mitochondrial extract of post-mortem patients' frontal cortex and age-matched control subjects or Q-7 or Q-111 cells (250 ng) or with purified recombinant PNKP (2 ng) was conducted as we described previously[20]. Five pmol of the radiolabeled substrate was incubated at 37°C for 15 min in buffer A (25 mM Tris-HCl, pH 8.0, 100 mM NaCl, 5 mM $MgCl_2$, 1 mM DTT, 10% glycerol and 0.1 µg/µl acetylated BSA).

5 pmol of non-radiolabeled substrate was used as cold substrate. For *in vitro* PNKP restoration, similar assays were done after incubation of F2,6BP/F6P/F1,6BP (in amounts as indicated in the figure legends) with the mitochondrial extracts for 15 min. The radioactive bands were visualized in PhosphorImager (GE Healthcare) and quantitated using ImageQuant software. The data were represented as % product (released phosphate or kinase product) released from the radiolabeled substrate with a value arbitrarily set at 100%.

Enzymatic preparation of F2,6BP

Enzymatic preparations of F2,6BP were conducted following the protocol as described before[20].

Estimation of F2,6BP in patients' extracts

The quantitation of F2,6BP from the purified mitochondrial extract of post-mortem patients was performed as described before[20].

Long amplicon quantitative PCR (LA-qPCR)

Genomic DNA was extracted from post-mortem tissues, striatal neuronal cells and Drosophila (10 each) using the Genomic tip 20/G kit (Qiagen) per the manufacturer's protocol, to ensure minimal DNA oxidation during the isolation steps. The DNA was quantitated by Pico Green (Molecular Probes) in a black-bottomed 96-well plate and gene-specific LA qPCR assays were performed as described earlier[20] using Long Amp Taq DNA Polymerase (New England BioLabs).

The amplified products were then visualized on gels and quantitated with ImageJ software (NIH). The extent of damage was calculated in terms of relative band intensity with a control/mock-treated sample or w^{1118} sample (for Drosophila studies) considered as 100. All oligos used in this study are listed below:

Oligo sets for amplification of mitochondrial fragment from mouse genome (Q-7 and Q-111 cells): For LA PCR: LA 1: 5′-GCC AGC CTG ACC CAT AGC CAT ATT AT-3′ LA 2: 5′-GAG AGA TTT TAT GGG TGT ATT GCG G-3′ For SA PCR: SA 1: -CCC AGC TAC TAC CAT CAT TCA AGT-3′ SA 2: 5′-GAT GGT TTG GGA GAT TGG TTG ATG-3′

Oligo sets for amplification of mitochondrial fragment from human genome (post-mortem patients): For LA PCR: LA 1: 5'- TCTAAGCCTCCTTATTCGAGCCGA-3' LA 2: 5'- TTTCATCATGCGGAGATGTTGGATGG-3' For SA PCR: SA 1: 5'-CCCCACAAACCCCATTACTAAACCCA-3' SA 2: 5'-TTTCATCATGCGGAGATGTTGGATGG-3'.

Oligo sets for amplification of mitochondrial fragment from Drosophila genome: For Fragment 1: LA 1: 5'-TGTGAATAATAGCCCCAGCACA-3' LA 2: 5'-GCTGGAATGAATGGTTGGACG-3' SA 1: 5'-ACACCTGCCCATATTCAACCA-3' SA 2: 5'-ACTGGTCGAGCTCCAATTCA-3'; For Fragment 2: LA 3: 5'-GTGAATAATAGCCCCAGCACA-3' LA 4: 5'-AGGCTGGAATGAATGGTTGGA-3' SA 3: 5'-ACCTGCCCATATTCAACCAGA-3' SA 4: 5'- TCAACTGGTCGAGCTCCAAT-3'.

***In cell* delivery of the exogenous F2,6BP/F1,6BP in Q-7 and Q-111 cells:**

For delivery of the glycolytic metabolites into the mouse striatum-derived neuronal cells (Q-7 and Q-111), we followed the protocol optimized in our lab[20]. Briefly, 200 μM of F2,6BP or F1,6BP was mixed with 25 μM cell-permeable carrier peptide K16ApoE (Mayo Proteomic Core Facility) and incubated for 45 min at RT; then

metabolite-peptide mix was added to the cells and incubated for 6 h in reduced serum (oPTIMEM) media. After 6 h, FBS containing complete media was added and cells were harvested at 72 and 96 h for DNA repair assays/LA-qPCR.

Antibodies and chemicals for immunostaining and flow cytometry

The antibodies and chemicals used for immunostaining were as follows: Mouse Anti-HTT Antibody-MW8 (Creative Biolab, San Diego, USA), Tetramethylrhodamine Methyl Ester Perchlorate (TMRM) from ThermoFischer scientific, USA, Thioflavin-T (Sigma-Aldrich, USA), DAPI (Novus, USA), NucRed dye (647) and MitoTracker from Invitrogem, USA).

FACS analysis

TMRM is widely used for assessing mitochondrial membrane potential due to its ability to accumulate within mitochondria in proportion to membrane potential, as predicted by the Nernst equation. The cells were grown on 10 cm cell culture dishes in DMEM at 37°C with 5% CO_2. The staining protocol was as follows:

Briefly, TMRM (1 μM) stock solution and Verapamil (2 nM) were mixed in a ratio of 2:1 and the cells were incubated in the staining solution for 1 hour at 37°C. Fluorescence intensity was measured by flow cytometry (FACSCalibur, BD Biosciences, CA, USA) using CellQuest Pro software (version 5.2, BD Biosciences, Franklin Lakes, NJ, USA). Each experiment was performed in duplicate.

Conflict of interest

The authors declare that they do not have any conflicts of interest.

Data availability

The data that support the findings of this study are available from the corresponding author upon request.

References:

1. H. Y. Zoghbi, H. T. Orr, Glutamine repeats and neurodegeneration. *Annu Rev Neurosci*. 23:217-47 **(2000).**
2. Genetic Modifiers of Huntington's Disease, C. Identification of Genetic Factors that Modify Clinical Onset of Huntington's Disease. *Cell* 162, 516-526, doi: 10.1016/j.cell.2015.07.003 **(2015).**
3. Genetic Modifiers of Huntington's Disease Consortium. Electronic address, g. h. m. h. e. & Genetic Modifiers of Huntington's Disease, C. CAG Repeat Not Polyglutamine Length Determines Timing of Huntington's Disease Onset. *Cell* 178, 887-900 e814, doi: 10.1016/j.cell.2019.06.036 **(2019)**.
4. R. A. Quintanilla, G. V. W. Johnson, Role of mitochondrial dysfunction in the pathogenesis of Huntington's disease. *Brain Res Bull* Oct 28;80(4-5):242-7 **(2009)**.
5. A. Jurcau, C. M. Jurcau, Mitochondria in Huntington's disease: implications in pathogenesis and mitochondrial-targeted therapeutic strategies. *Neural Regen Res* Jul;18(7):1472-1477 **(2023)**.
6. A. Neueder et al. Huntington's disease affects mitochondrial network dynamics predisposing to pathogenic mitochondrial DNA mutations. *Brain* Jun 3;147(6):2009-2022 **(2024)**.

7. E. Martin-Solana et al. Disruption of the mitochondrial network in a mouse model of Huntington's disease visualized by in-tissue multiscale 3D electron microscopy. *Acta Neuropathol Commun* Jun 5;12(1):88 **(2024)**.
8. I. Shokolenko et al. Oxidative stress induces degradation of mitochondrial DNA. *Nucleic Acids Res* May;37(8):2539-48 **(2009)**.
9. K. Acevedo-Torres et al. Mitochondrial DNA damage is a hallmark of chemically induced and the R6/2 transgenic model of Huntington's disease. *DNA Repair (Amst)* Jan 1;8(1):126-36 **(2009)**.
10. S. Ayala-Peña Role of oxidative DNA damage in mitochondrial dysfunction and Huntington's disease pathogenesis. *Free Radic Biol Med*. Sep:62:102-110 **(2013)**.
11. A. Siddiqui et al. Mitochondrial DNA damage is associated with reduced mitochondrial bioenergetics in Huntington's disease. *Free Radic Biol Med*. Oct 1;53(7):1478-88 **(2012)**.
12. L. Weissman et al. DNA repair, mitochondria, and neurodegeneration. *Neuroscience* Apr 14;145(4):1318-29 **(2007)**.
13. A. Jilani, et al., Molecular cloning of the human gene, PNKP, encoding a polynucleotide kinase 3'-phosphatase and evidence for its role in repair of DNA strand breaks caused by oxidative damage. *J Biol Chem* Aug 20;274(34):24176-86 **(1999)**.
14. F. Karimi-Busheri, et al., Molecular characterization of a human DNA kinase. *J Biol Chem* Aug 20;274(34):24187-94 **(1999)**.
15. M. Shimada, L. C. Dumitrache, H. R. Russell, P. J. McKinnon, Polynucleotide kinase-phosphatase enables neurogenesis via multiple DNA repair pathways to maintain genome stability. *Embo Journal* 34, 2465-2480, doi:10.15252/embj.201591363 **(2015)**.
16. J. Shen, et al., Mutations in PNKP cause microcephaly, seizures and defects in DNA repair. *Nat Genet* 42, 245-249 **(2010)**.
17. C. Poulton, et al., Progressive cerebellar atrophy and polyneuropathy: expanding the spectrum of PNKP mutations. *Neurogenetics* 14, 43-51 **(2013)**.
18. A. Islam, et al., Functional analysis of a conserved site mutation in the DNA end processing enzyme PNKP leading to ataxia with oculomotor apraxia type 4 in humans. *J Biol Chem* 299, 104714 **(2023)**.
19. R. Gao, et al., Mutant huntingtin impairs PNKP and ATXN3, disrupting DNA repair and transcription. *Elife* 8, doi:10.7554/eLife.42988 **(2019)**.
20. A. Chakraborty et al. Fructose-2,6-bisphosphate restores DNA repair activity of PNKP and ameliorates neurodegenerative symptoms in Huntington's disease. *Proc Natl Acad Sci USA* Sep 24;121(39):e2406308121 **(2024)**.
21. J. Hu et al. Repair of formamidopyrimidines in DNA involves different glycosylases: role of the OGG1, NTH1, and NEIL1 enzymes. *J Biol Chem* Dec 9;280(49):40544-51 **(2005)**.
22. S. M. Mandal et al. Role of human DNA glycosylase Nei-like 2 (NEIL2) and single strand break repair protein polynucleotide kinase 3'-phosphatase in maintenance of mitochondrial genome. *J Biol Chem*. Jan 20;287(4):2819-29 **(2012)**.
23. N. Tahbaz et al. Role of polynucleotide kinase/phosphatase in mitochondrial DNA repair. *Nucleic Acids Res* Apr;40(8):3484-95 **(2012)**.

24. A. Chakraborty, et al., Classical non-homologous end-joining pathway utilizes nascent RNA for error-free double-strand break repair of transcribed genes *Nature communications* 7, 13049, doi:10.1038/ncomms13049 **(2016)**.
25. E. Romero, et al., Suppression of neurodegeneration and increased neurotransmission caused by expanded full-length huntingtin accumulating in the cytoplasm. *Neuron* Jan 10;57(1):27-40 **(2008)**.
26. F. Trettel, et al., Dominant phenotypes produced by the HD mutation in STHdh(Q111) striatal cells. *Human molecular genetics* 9:2799-809 **(2000)**.
27. M. Z. Chen et al. N-Terminal Fragments of Huntingtin Longer than Residue 170 form Visible Aggregates Independently to Polyglutamine Expansion. *J Huntingtons Dis* ;6(1):79-91 **(2017)**.
28. S. J. Tabrizi et al. Huntington disease: new insights into molecular pathogenesis and therapeutic opportunities. *Nat Rev Neurol* Oct;16(10):529-546 **(2020)**.
29. C. M. Diaz-Garcia, et al., Neuronal Stimulation Triggers Neuronal Glycolysis and Not Lactate Uptake. *Cell Metab* 26, 361-374 e364, doi:10.1016/j.cmet.2017.06.021 **(2017).**
30. K. H. Kim, C. B. Lee, Socialized mitochondria: mitonuclear crosstalk in stress. *Exp Mol Med* May;56(5):1033-1042 **(2024)**.
31. Z. Xun, et al., Targeting of XJB-5-131 to mitochondria suppresses oxidative DNA damage and motor decline in a mouse model of Huntington's disease. *Cell Rep* Nov 29;2(5):1137-42 **(2012)**.
32. P. Wipf, et al., A Double-Pronged Sword: XJB-5-131 Is a Suppressor of Somatic Instability and Toxicity in Huntington's Disease. *J Huntingtons Dis* 11(1):3-15 **(2022)**.

Acknowledgement

This work was supported by National Institute of Health Grants 2R01 NS073976 and R56NS073976 to TH, R01AI163327 and R21 AG078635 to GG, Don and Nancy Mafrige Professorship in Neurodegenerative Diseases (BK), Alzheimer's Association Research Grant (AARG-17-533363 BK), National Institutes of Aging (R21-AG059223 and R01-AG063945 BK), National Institute of Health grant RF1NS112719 to MLH. We thank the Michigan Brain Bank (5P30 AG053760 University of Michigan Alzheimer's Disease Core Center) for providing us with the tissue of post-mortem HD patients and their age-matched controls.

Figures and Legends

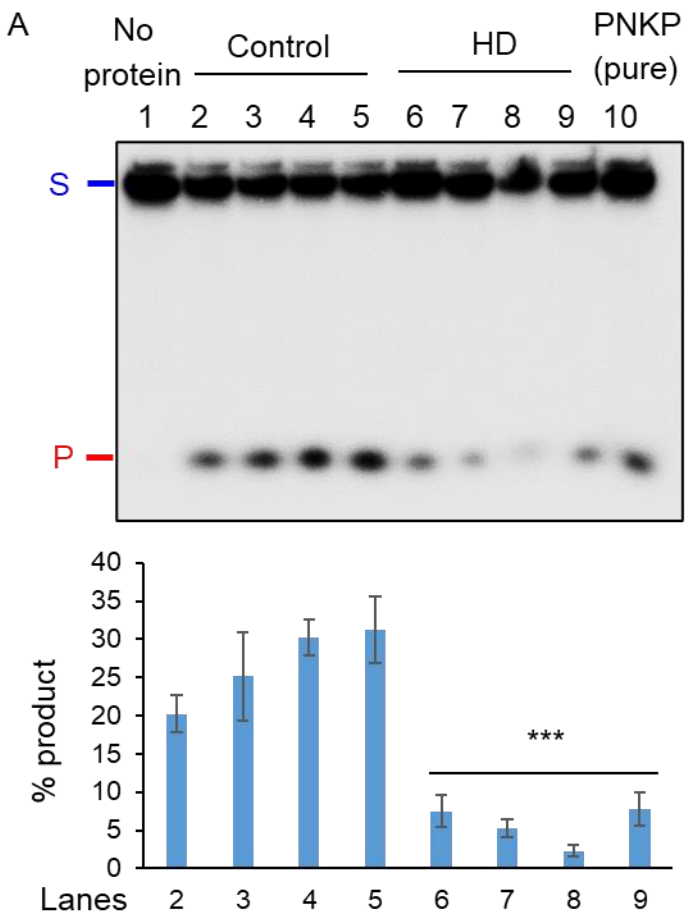

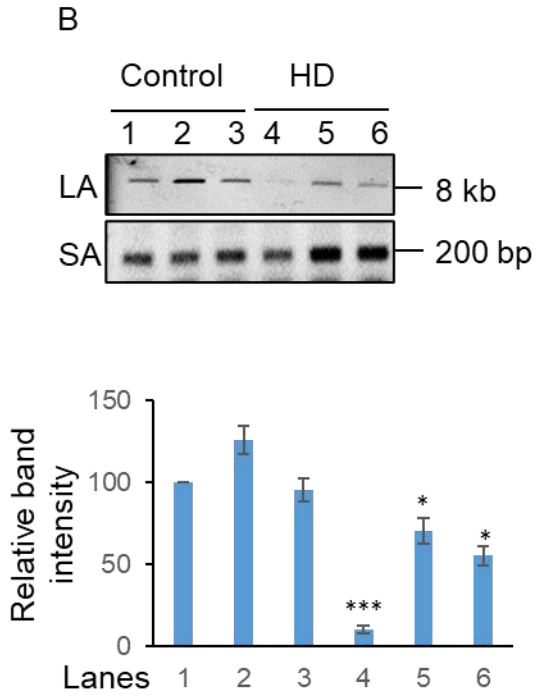

Figure 1: A. Upper panel: 3'-phosphatase activity of PNKP in the mitochondrial extract (250 ng) of frontal cortex from healthy normal control (lanes 2-5) vs. age-matched HD patients (lanes 6-9). Lane 1: substrate only. Lane

10: Purified PNKP (2 ng). S: Substrate and P: Released phosphate. Lower panel: Quantitation of the % released phosphate in the indicated lanes; error bars represent mean ± SD. ***P<0.005 between Control vs. HD patient. **B.** Upper panel: Representative agarose gel image of long (LA) and short (SA) amplicon of the mitochondrial fragment from genomic DNA of postmortem frontal cortex of age-matched healthy normal (control) (lanes 1-3) and HD patients (lanes 4-6). Lower panel: The normalized relative band intensities are represented in the bar diagram with one control sample arbitrarily set as 100. The damage accumulation in HD patients was significantly increased (***P < 0.005; *P < 0.05).

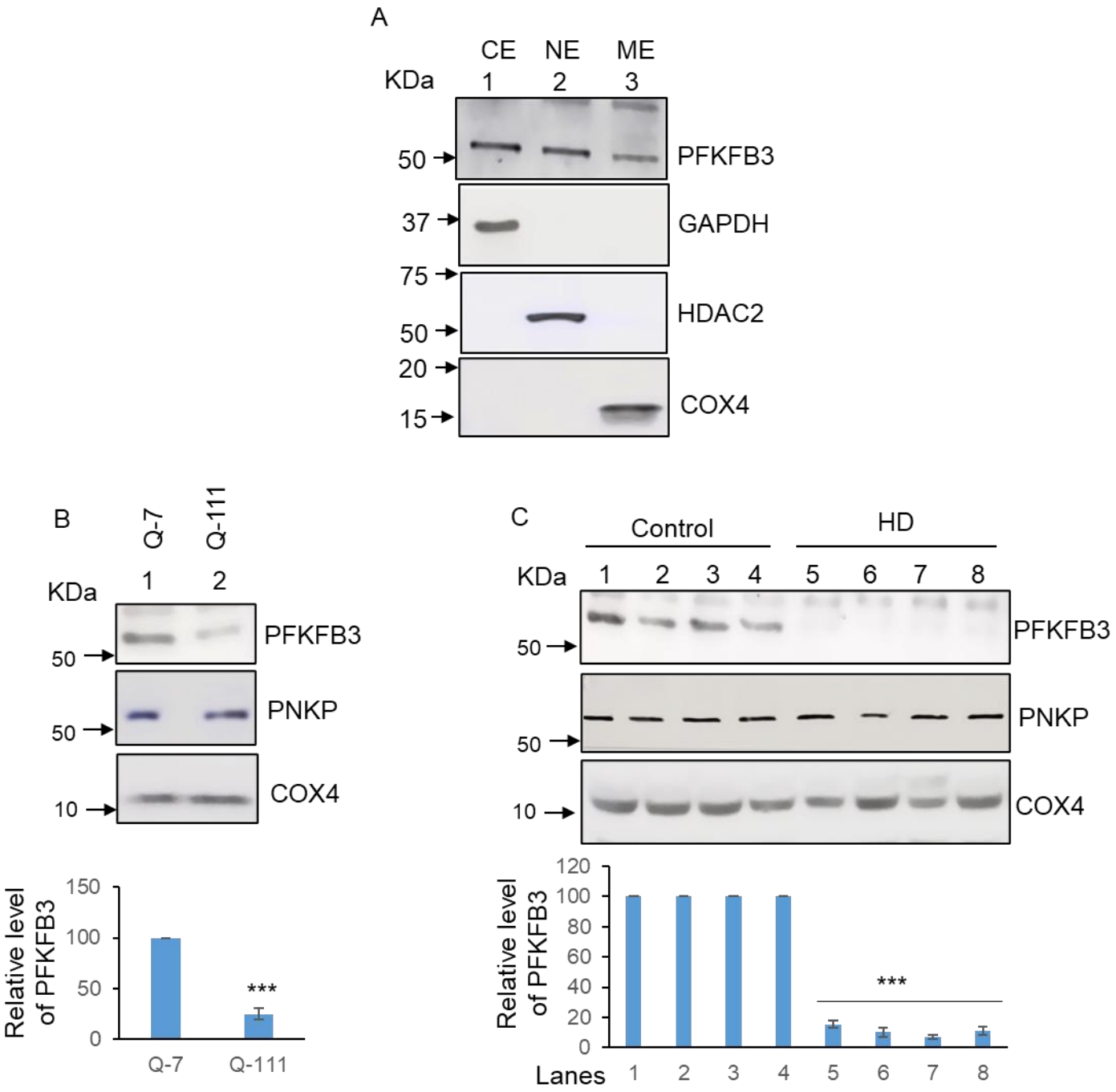
A
CE
NE
ME
KDa
1
2
3
50
PFKFB3
37
GAPDH
75
HDAC2
50
20
COX4
15
B
Q-7
Q-111
KDa
1
2
50
PFKFB3
50
PNKP
10
COX4
Relative level of PFKFB3
150
100
50
0
***
Q-7
Q-111
C
Control
HD
KDa
1 2 3 4 5 6 7 8
50
PFKFB3
50
PNKP
10
COX4
Relative level of PFKFB3
120
100
80
60
40
20
0
***
Lanes
1 2 3 4 5 6 7 8

D

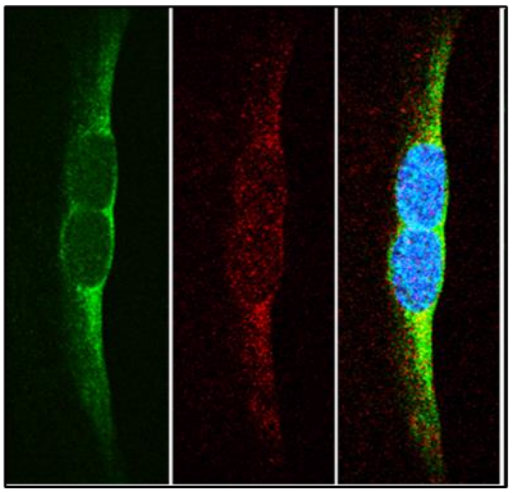

Mito PFKFB3 Overlay

Q-7

E

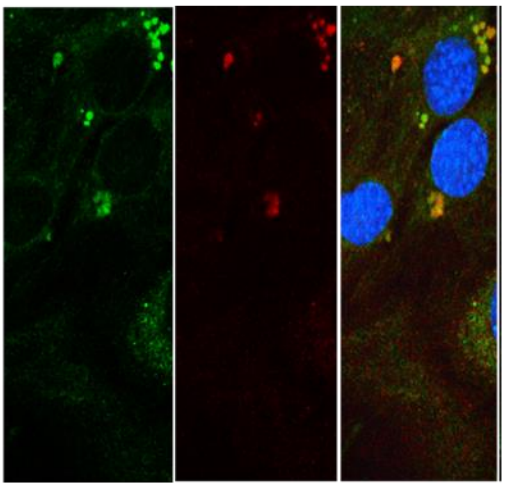

Mito PFKFB3 Overlay

Q-111

F

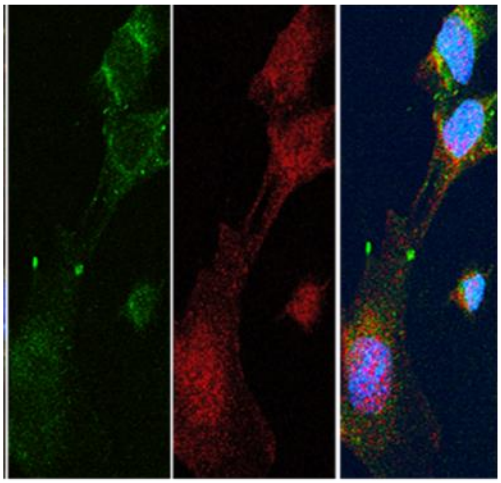

Mito PFKFB3 Overlay

Q-111+F2.6BP

G

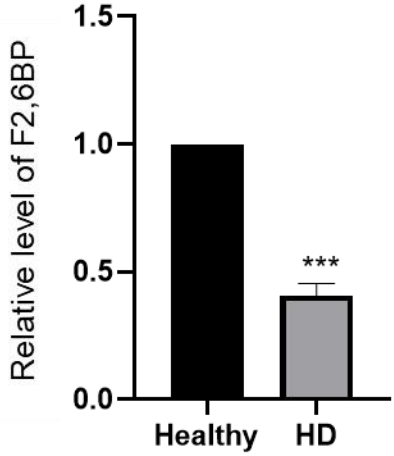

Figure 2: A. Western blot showing the relative levels of PFKFB3 in the cytosolic (CE), nuclear (NE) and mitochondrial (ME) extract of HEK293 cells. GAPDH: cytosolic loading control; HDAC2: nuclear loading control. COX4: mitochondrial loading control. **B.** Western blot showing the relative levels of PNKP and PFKFB3 in the mitochondrial extract of Q-7 and Q-111 cells. COX4: mitochondrial loading control. Lower panel: Quantitation of the relative PFKFB3 levels after normalization with loading control COX4 (***P<0.005). **C.** Western blot showing the relative levels of PNKP and PFKFB3 in the mitochondrial extract of HD patients vs. age-matched control subjects' frontal cortex. COX4: mitochondrial loading control. Lower panel: Quantitation of the relative PFKFB3 levels after normalization with loading control COX4 (***P<0.005). **D-F:** Q-7 **(D)** and Q-111 **(E)** cells were first stained with MitoTracker dye, which marks mitochondria in green (left panels), followed by fixation and staining for PFKFB3 using a secondary antibody conjugated to Alexa Fluor 568, giving a cherry red signal (middle panels). The overlap of these signals appears yellow in merged images (right panels), confirming PFKFB3's mitochondrial localization. **(F)** Represents Q-111 cells after treatment with F2,6BP, showing improved co-localization in the merged image suggesting that F2,6BP may help restore mitochondrial integrity and PFKFB3 levels in Q-111 cells. Nuclei is counterstained with DAPI. **(G)** Bar diagram showing the relative levels of F2,6BP in the mitochondrial extract of control vs. HD patients' frontal cortex (***P<0.005).

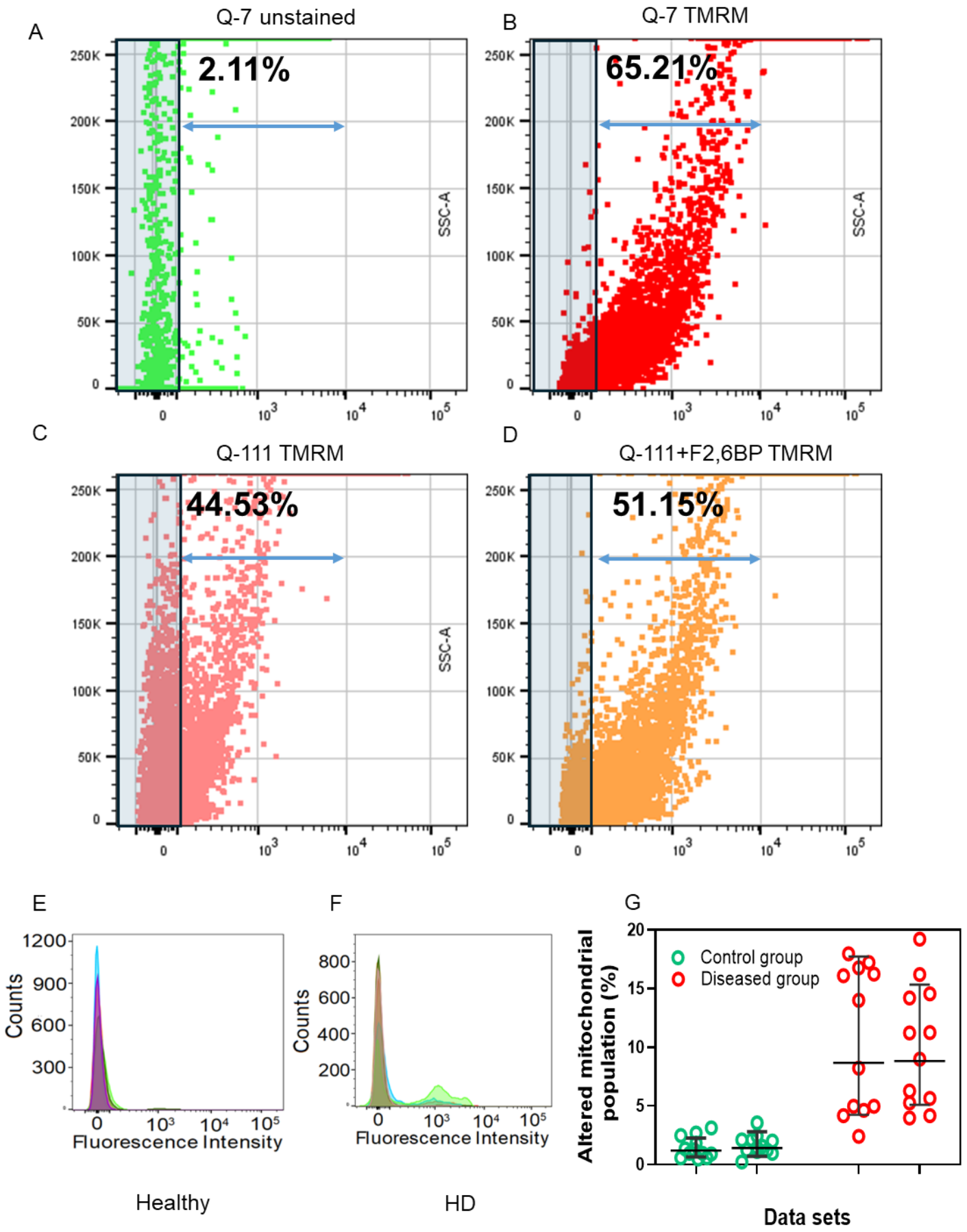

Figure 3: A-D: Flow cytometry scatter plot analysis illustrates changes in mitochondrial membrane potential in

Q-7 cells without TMRM **(A)**, Q-7 cells with TMRM **(B)**, Q-111 cells with TMRM **(C)**, and F2,6BP-treated Q-111 cells with TMRM **(D)**. Fluorescence intensity of TMRM was measured using the PE channel. **(E-G)** Isolated mitochondria from both healthy and HD tissues were analyzed by FACS using the MitoView™650 dye on the PE channel, revealing distinct populations with different mitochondrial percentages. Mitochondria from diseased tissues **(F)** demonstrated a separate population compared to mitochondria from control tissues **(E)**. Quantitative results from duplicate analyses are summarized in the bar graph **(G)** and are expressed as mean ± SE.

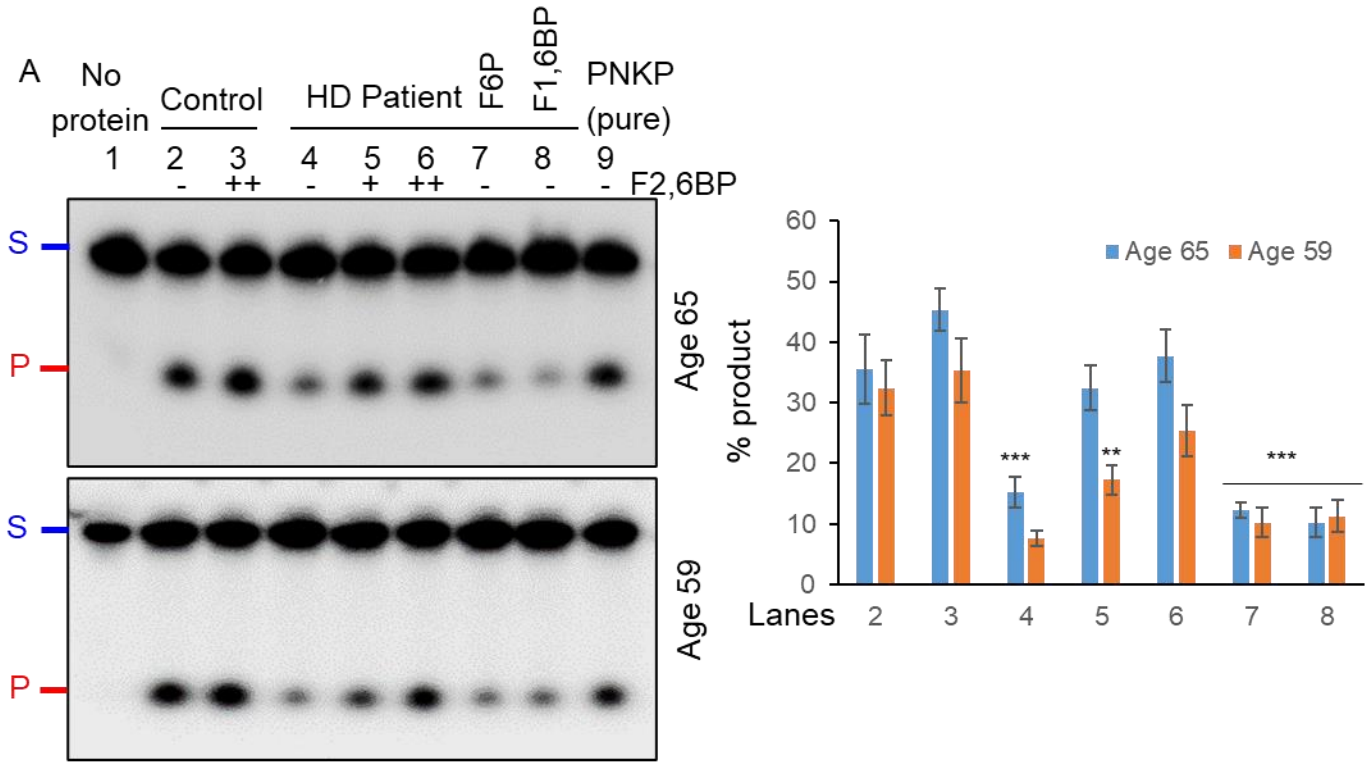

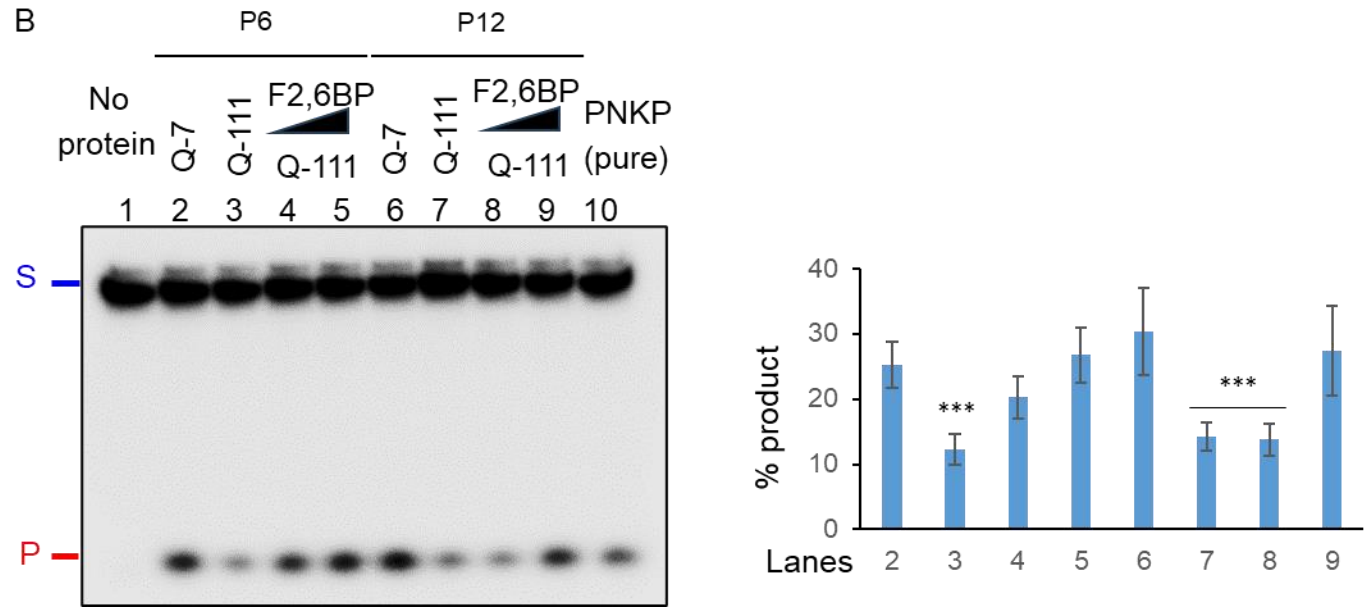

Figure 4: A. Left panel: Representative gel images (two different age-groups) showing the 3'-phosphatase activity of PNKP in the post-mortem brain (frontal cortex) mitochondrial extract of healthy normal control (lane 2) or supplemented with F2,6BP (lane 3, 50 μM), and age/gender-matched HD patient (lane 4) or supplemented with F2,6BP (lanes 5-6, 25 and 50 μM) or F6P (lane 7, 50 μM) or F1,6BP (lane 8, 50 μM). Lane 1: substrate only. Lane 9: purified PNKP (1-2 ng). S: Substrate and P: Released phosphate. Right panel: Quantitation of the % released phosphate in the indicated lanes (***P<0.005; **P<0.01). **B.** Left panel: Representative gel image showing the 3'-phosphatase activity of PNKP in the mitochondrial extract of Q-7 cells (lanes 2, 6) and Q-111 cells

(lanes 3, 7) or Q-111 cells supplemented with F2,6BP (lanes 4-5 and 8-9, 25-50 μM). Lane 1: substrate only. Lane 10: purified PNKP (1-2 ng). S: Substrate and P: Released phosphate. Cells from two different passages are used (P6 and P12). Right panel: Quantitation of the % released phosphate in the indicated lanes (***P<0.005, between Q-7 and Q-111 cells).

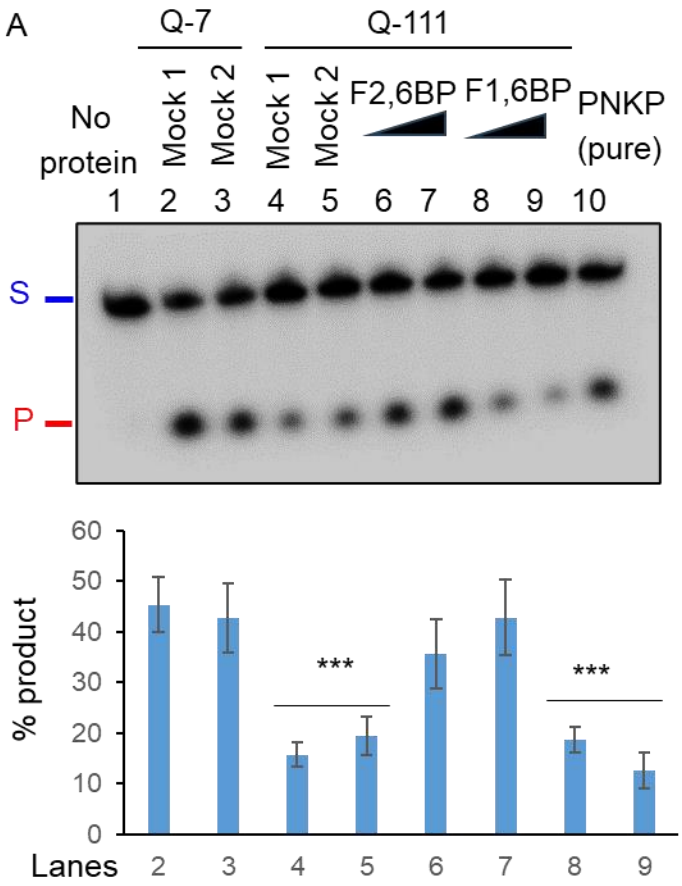
A
Q-7
Q-111
No protein
Mock 1
Mock 2
Mock 1
Mock 2
F2,6BP
F1,6BP
PNKP (pure)
1 2 3 4 5 6 7 8 9 10
S
P
% product
60
50
40
30
20
10
0
***
***
Lanes 2 3 4 5 6 7 8 9

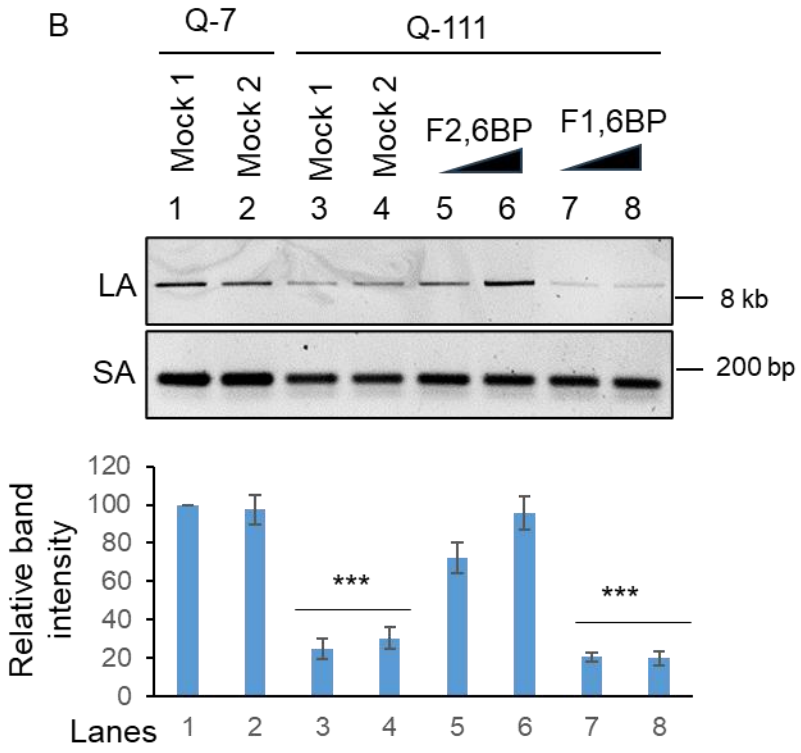
B
Q-7
Q-111
Mock 1
Mock 2
Mock 1
Mock 2
F2,6BP
F1,6BP
1 2 3 4 5 6 7 8
LA
SA
8 kb
200 bp
Relative band intensity
120
100
80
60
40
20
0
***
***
Lanes 1 2 3 4 5 6 7 8

C

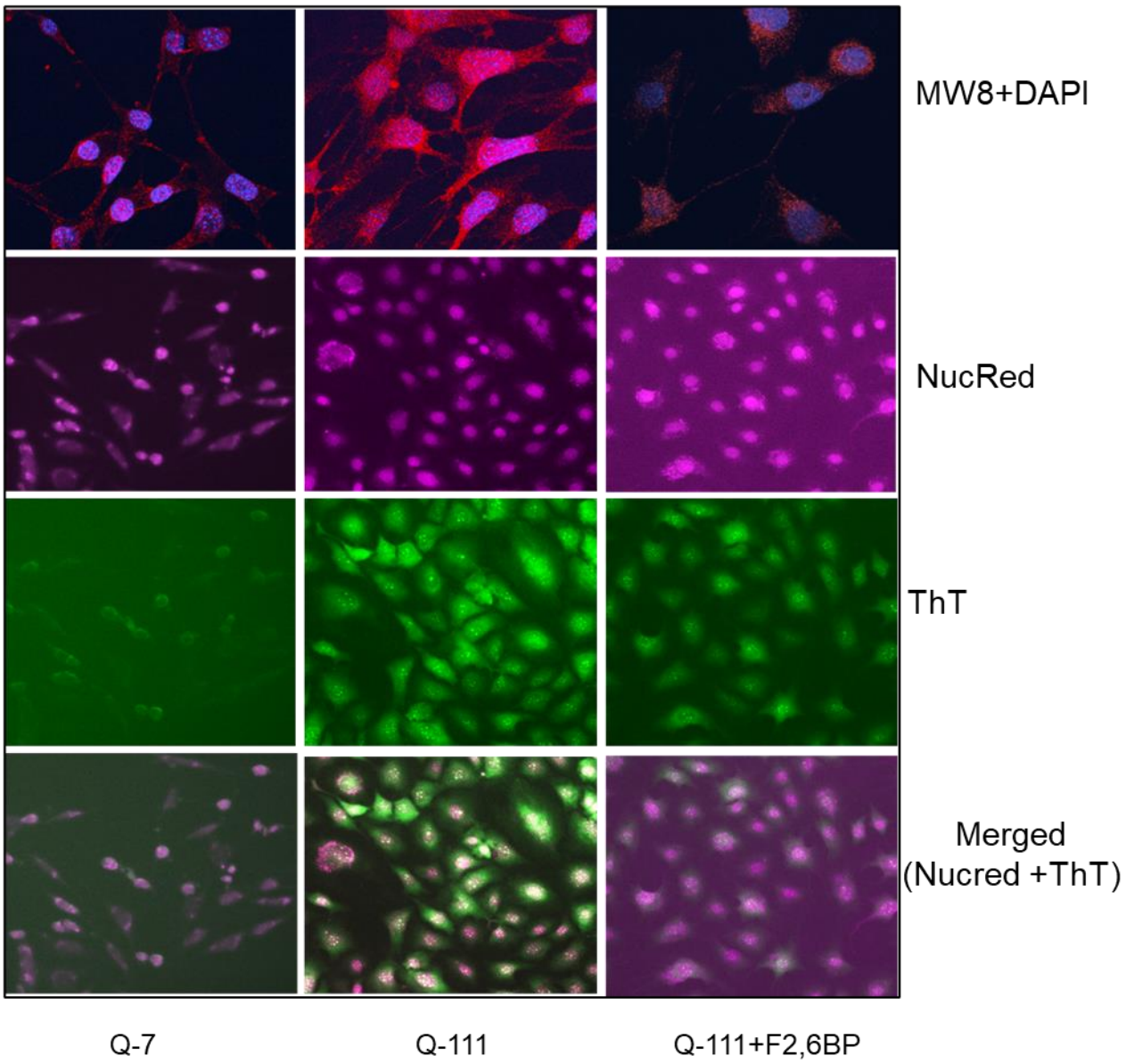

Figure 5: A. Upper panel: Representative gel image of 3'-phosphatase activity of PNKP in the mitochondrial extract of Q-7 (lanes 2-3) and Q-111 (lanes 4-9) cells with mock treatment (Mock 1; lanes 2 and 4), treatment with K16ApoE carrier peptide alone (25 μM; Mock 2; lanes 3 and 5) or supplemented with F2,6BP (200 μM; 72 and 96 h) (lanes 6-7), or F1,6BP (lanes 8-9, 200 μM) in presence of carrier peptide. Lane 1: substrate only. Lane 10: purified PNKP (2 ng). Lower panel: Quantitation of the % released phosphate in the indicated lanes. Error bars show ±SD of the mean; ***P<0.005 compared to lanes 2, 3. **B.** Upper panel: Amplification of long amplicon (LA) and a short amplicon (SA) of the mitochondrial fragment to assess DNA strand break accumulation. Lower panel: The bar diagram represents the normalized (with short amplicon) relative band intensity with the mock-treated Q-7 sample arbitrarily set as 100. **C.** (Top) Immunofluorescence micrographs show HTT expression and aggregation in Q-7 (left), Q-111 (middle) and Q-111 cells treated with F2,6BP (right). Cells were stained with Anti-HTT Antibody MW8, visualized using a mouse secondary antibody conjugated to Alexa Fluor™568, resulting in red fluorescence. The nuclei were counter stained with DAPI. Images were captured at 600X magnification using

a SoRa super-resolution spinning disk confocal system with motorized FRAP/photobleaching. (Remaining three panels) Aggregation levels were assessed with ThT dye, which fluoresces green, and nuclear localization was indicated by NucRed dye, providing a cyan signal in the images. Imaging was performed on the EVOS™ M5000 system at 200X magnification.

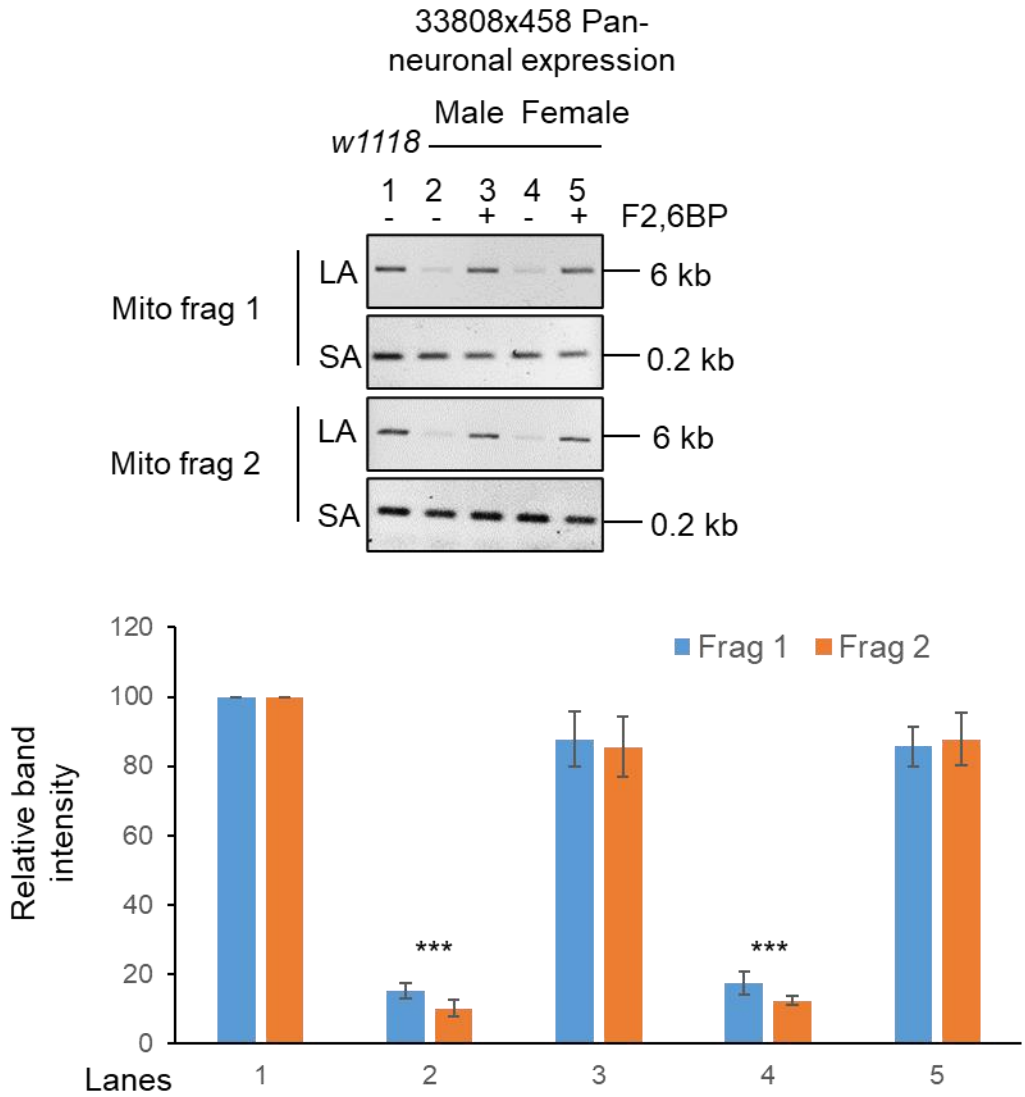

Figure 6: Upper panel: Representative agarose gel images of long (LA) and short (SA) amplicon of the two mitochondrial fragments from genomic DNA of male (lanes 2-3) and female (lanes 4-5) flies with pan-neuronal expression of *Htt*128Q either mock-treated (lanes 2 and 4) or treated with F2,6BP (lanes 3 and 5). Lane 1: *w1118* (males and females). Lower panel: The normalized relative band intensities were represented in the bar diagram with *w1118* arbitrarily set as 100 (error bars represent ±SD of the mean). The damage for each gene in Drosophila pan-neuronal expression of *Htt*128Q was significant (***P<0.005) compared to the *w1118* samples. Also, the strand breaks were significantly repaired in F2,6BP-treated samples.